Switchable resonant hyperpolarization transfer to ^{29}Si spins in natural silicon

Phillip Dluhy,[1] Jeff Z. Salvail,[1] Kamyar Saeedi,[1] Mike L. W. Thewalt,[1] and Stephanie Simmons[2,*]
[1]*Department of Physics, Simon Fraser University, Burnaby, BC, Canada V5A 1S6*
[2]*Department of Materials, Oxford University, Oxford OX1 3PH, United Kingdom*

(Received 23 September 2014; revised manuscript received 21 April 2015; published 26 May 2015)

Silicon nano- and microparticles containing polarized ^{29}Si spins are promising inexpensive and biocompatible medical imaging agents, particularly for magnetic resonance imaging (MRI). Maximizing out-of-equilibrium polarization (i.e., hyperpolarization) of the ^{29}Si nuclear spins as efficiently as possible is critical for such an application. Here we identify and exploit a frequency-matched resonant transfer process between easily hyperpolarized bulk ^{31}P and otherwise insensitive ^{29}Si nuclear spins in natural silicon, boosting the ^{29}Si signal to over 200 times its thermal equilibrium signal. This technique could be used in tandem with microwave-based hyperpolarization schemes for even higher efficiencies. Lastly, this hyperpolarization buildup process does not necessarily introduce an additional source of decoherence; after hyperpolarization the resonant transfer process can be switched off to recover the ultralong lifetimes of ^{29}Si spins for *in vivo* imaging.

DOI: 10.1103/PhysRevB.91.195206 PACS number(s): 75.76.+j, 75.40.Gb, 71.35.−y, 76.60.−k

Magnetic resonance imaging (MRI) is widely used for medical diagnosis because of its high spatial resolution, sensitivity, and noninvasive nature [1]. The MRI signal relies on the existence of polarized nuclear spins, but the small equilibrium polarization of nuclear spins necessitates either large magnetic fields, yielding polarizations on the order of 10^{-5} at room temperature, or injecting highly spin polarized imaging agents that can be imaged more quickly and with greater spatial resolution using cost-effective, low-field magnets [2,3]. Hyperpolarized imaging agents require both a source of hyperpolarization to transfer to the target nuclei as well as long spin lifetimes (T_1) to sustain nuclear hyperpolarization *in vivo* throughout the imaging procedure [1,3].

The notably long T_1 times of ^{29}Si in silicon, exceeding hours at room temperature [4], as well as its biocompatibility and low background signal in the body, make it a promising candidate for direct, high contrast MRI *in vivo* [1]. The thermal polarization of unpaired electron spins—associated with donors [5,6], conduction band electrons [7,8], or surface dangling bonds [3,9,10]—is a well-studied source of ^{29}Si hyperpolarization [5,11]. However, introducing a large number of these unpaired electrons to hyperpolarize the ^{29}Si spins simultaneously reduces their T_1 lifetimes [10]. It is therefore of interest to identify a switchable source of hyperpolarization for the ^{29}Si spins so that after the hyperpolarization procedure is complete, the coupling can be turned off to recover long T_1 times.

When employing unpaired electrons to directly hyperpolarize the ^{29}Si, spin polarization transfer occurs via the relatively slow solid or Overhauser effect processes that rely on the direct interaction between an electron and a ^{29}Si nuclear spin resulting in the mutual flip of each spin, referred to as zero-quantum ($\Delta m_s = \pm 1, \Delta m_I = \mp 1$) or double-quantum ($\Delta m_s = \pm 1, \Delta m_I = \pm 1$) transitions [12]. The solid effect occurs when these transitions are driven directly [12], whereas the Overhauser effect occurs when the electrons are held out of equilibrium and zero- or double-quantum relaxation processes transfer the electron polarization to the nuclear spins [5]. These transitions are only weakly allowed via the relatively small hyperfine interaction of unpaired electrons with the ^{29}Si nuclear spins [13]. Hence, the effectiveness of directly hyperpolarizing the ^{29}Si using the solid or Overhauser effect decreases with increasing magnetic field and has a maximum polarization that is limited by the thermal electron polarization [12].

In contrast, at low temperatures, dilute donor nuclear spins in silicon, such as ^{31}P, support a number of efficient nuclear hyperpolarization mechanisms, including bound exciton optical methods [14], broadband optical processes [15], pulsed techniques [16], and a faster Overhauser process made possible by the much stronger hyperfine interaction [17]. Although the low concentration and temperature limitations of neutral ^{31}P nuclear spins make them unsuitable as hyperpolarized nuclei for direct MRI, they can act as an efficient reservoir of hyperpolarization for host ^{29}Si spins provided one can promote efficient spin diffusion between ^{31}P and ^{29}Si nuclear spins.

The key to our switchable ^{29}Si hyperpolarization scheme is in the fact that there exists a magnetic field and electron spin state where the ^{31}P nuclear spin frequency matches that of the bulk ^{29}Si spins: a "resonant matching field condition." Phosphorus donor spins are described by the spin Hamiltonian $\mathcal{H}_0 = \omega_e S_z - \omega_I I_z + A \cdot \vec{S} \cdot \vec{I}$, where $\omega_e = g\beta B_0/\hbar$ and $\omega_I = g_I \beta_n B_0/\hbar$ are the electron and nuclear Zeeman frequencies, g and g_I are the electron and nuclear g factors [18], β and β_n are the Bohr and nuclear magnetons, and B_0 is the magnetic field applied along the z axis in the laboratory frame. The large hyperfine interaction constant $A = 117.53$ MHz splits the ^{31}P nuclear resonance frequencies according to the state of the electron spin. For the electron spin-up configuration ($|\uparrow\rangle$), the transition frequency of the ^{31}P nuclei is calculated to match that of the bulk ^{29}Si spins (assuming a gyromagnetic ratio of -8.458 MHz/T [13]) at 19.315 MHz under an applied magnetic field near 2.2836 T (see Fig. 1). The resonant dipolar spin diffusion between the ^{31}P and ^{29}Si spins can be easily switched off: spin diffusion is significantly suppressed at other magnetic fields where the transition frequencies are far off resonance.

To exploit the resonant matching condition to hyperpolarize the ^{29}Si, we first hyperpolarize the ^{31}P nuclear spins by

*Present address: CQC2T, Electrical Engineering Department, UNSW, Sydney, Australia; stephanie.simmons@unsw.edu.au

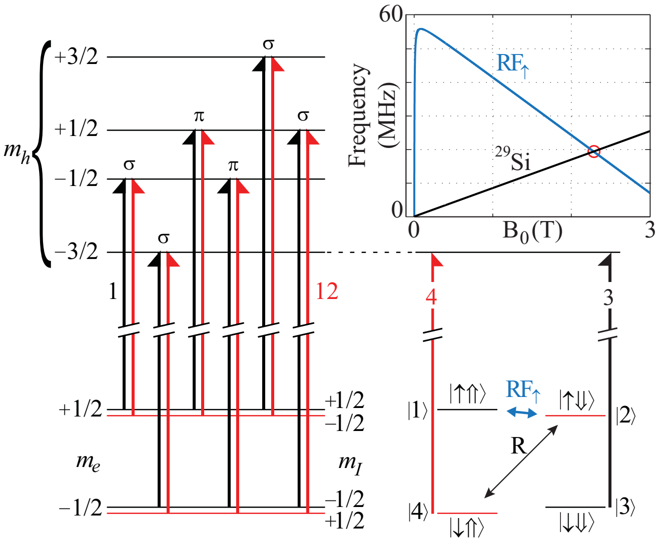

FIG. 1. (Color online) Nuclear hyperpolarization and transfer scheme. Left: The 12 bound exciton transitions (top) starting from the neutral ground state of ^{31}P donors in silicon (bottom). In natural silicon these isotopically broadened transitions allow for electron spin-selective ionization (but not nuclear spin-selective ionization) through Auger recombination. Right: Driving transitions 3 and 4 simultaneously pumps neutral donors into the electron spin-up state (|↑⟩). The cross relaxation (R) generates nuclear hyperpolarization via an Overhauser process. Inset: Nuclear resonance frequencies of ^{29}Si spins and the electron |↑⟩ branch of neutral ^{31}P donors. A resonant matching condition occurs near 2.28 T at a frequency near 19.3 MHz.

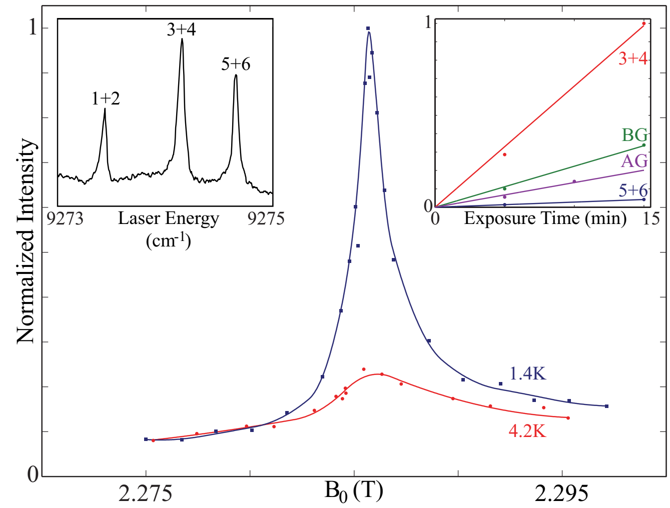

FIG. 2. (Color online) Resonant hyperpolarization transfer. Center: Total integrated NMR-detected ^{29}Si signal taken at a range of magnetic fields, each after 5 min of optical pumping of transitions 3 and 4. The magnetic field is inferred from the NMR-matched resonant bulk ^{29}Si frequency. A ^{29}Si frequency of 19.332 MHz, corresponding to a static field of 2.2856 T, allows for peak resonant hyperpolarization transfer. Magnetic field positions were ordered stochastically and nuclear polarization was erased between points. Amplitude errors are approximately the size of the points, and the solid line is a guide to the eye. Left inset: Q factor detected bound exciton transitions 1–6. Right inset: ^{29}Si signal intensity for exposure times from 5 to 15 min at 2.2856 T when pumping lines 3 and 4, lines 5 and 6, nonresonant below-gap (BG) (9275.08 cm^{-1}) excitation, and above-gap (AG) 1047 nm (∼9551cm^{-1}) excitation.

optically pumping bound exciton transitions at low temperatures [19] as shown in Fig. 1. In natural silicon at 1.4 K and near 2.28 T, the optical linewidths of the resonant bound exciton transitions are narrow enough to selectively excite a particular electron spin state. We create bound excitons conditional upon the donor electron being spin down (|↓⟩) by pumping bound exciton transitions 3 and 4, as labeled in Fig. 1. The bound exciton decays through Auger recombination, leaving the donor ionized and populating the conduction band with high spin temperature electrons. An electron |↓⟩ neutralization event restarts the bound exciton creation and decay cycle, whereas an electron |↑⟩ neutralization event brings the donor out of optical resonance. This effectively pumps electron polarization to the |↑⟩ state, allowing any ^{31}P nuclear hyperpolarization to couple and diffuse out to the ^{29}Si. Creating an inverted electron spin temperature while using low temperatures to generate a large thermal Boltzmann polarization across the zero quantum transition (R) efficiently drives an enhanced nuclear Overhauser effect that has the potential to generate a ^{31}P hyperpolarization that goes beyond the thermal electron polarization.

We tested this process using a $1 \times 1 \times 1$ cm^3 n-type natural silicon sample with a ^{31}P concentration of $\sim 6 \times 10^{15}$ cm^{-3}. To determine the optical frequencies that correspond to bound exciton (D^0X) transitions 3 and 4, we mount the sample in a 20 turn solenoid coil matched to 50 Ω, tune it to the ^{29}Si resonant frequency, and scan a single-frequency laser across the six lowest energy D^0X transitions. Similar to the "contactless EDMR" readout technique [20,21], when the laser comes into optical resonance with one of the D^0X transitions it creates a large number of carriers in the sample, changing its resistivity, which we detect by monitoring the change in the Q factor of the resonant cavity. This conveniently allows us to detect both the narrow-linewidth optical resonances as seen in Fig. 2 and later the ^{29}Si NMR signal using the same resonator hardware. In this sample, the D^0X optical linewidths are ∼2.5 GHz forcing us to dither the laser frequency (∼1.8 GHz) over the center of the measured optical resonance of lines 3 and 4 to improve the electron spin inversion.

To detect resonant hyperpolarization transfer, we tune the same resonant NMR circuit to the ^{29}Si nuclear resonance frequency at a range of fields centered on the matching field near 2.28 T and directly detect the ^{29}Si NMR signal after 5 min of hyperpolarization at each point. Results are shown in Fig. 2. After each free induction decay measurement the ^{29}Si spin polarization is reset to zero by applying a very long resonant radio frequency pulse tuned to the ^{29}Si frequency.

The overall ^{29}Si polarization near the matching field condition varies with temperature. At pumped LHe temperatures, the larger electron polarization (∼0.80 at 1.4 K versus ∼0.35 at 4.2 K) produces a larger Overhauser nuclear hyperpolarization of the ^{31}P spins. Additionally, the longer T_1 of the electron spins at lower temperatures produces a larger steady-state electron inversion, which in turn puts more ^{31}P nuclear spins in resonance with the ^{29}Si nuclear spins. Any further temperature-dependent contributions to the observable ^{29}Si hyperpolarization are likely due to nonresonant processes. In particular, the doubly occupied D^- donor electron singlet charge state becomes weakly bound at these lowest temperatures, and can conceivably affect the hyperpolarization dynamics.

The linewidth, peak position, and peak asymmetry observed in Fig. 2 are due to the distribution of ^{29}Si centers around the phosphorus donors, which gives rise to an inhomogeneous distribution of matching field conditions. This asymmetry is independent of the magnetic field sampling order and is due to the small anisotropic hyperfine interaction between ^{31}P donor electrons and the ^{29}Si spins [13,22]. This effect forms a "diffusion barrier" which slows the rate of hyperpolarization transfer by detuning the closest, highly coupled ^{29}Si spins relative to the unshifted bulklike ^{29}Si spins [23].

The highly coupled ^{29}Si spins within the diffusion barrier have matching field conditions higher than the peak position of 2.2856 T, and at these fields the rate-limiting spin diffusion step is between ^{29}Si spins on opposing sides of the diffusion barrier. Contrarily, the weakly coupled ^{29}Si spins far outside the diffusion barrier have matching field conditions at lower field values, closer to the bulk ^{29}Si matching field condition calculated to be at 2.2836 T, and at these fields the rate-limiting spin diffusion step is the slow flip-flop rate between distant ^{29}Si and ^{31}P spins. The peak occurs at a field slightly shifted from the calculated bulk ^{29}Si matching field condition, where the ^{31}P spins are resonant with the ^{29}Si spins on the "edge" of the diffusion barrier, promoting the most efficient spin diffusion to the bulk. This peak position is a function of both the number of available ^{29}Si spins at a given hyperfine coupling strength as well as the balance of diffusion rates from ^{31}P to the inner ^{29}Si and between the inner and bulklike ^{29}Si spins.

We can choose to create cold, hot, or negative electron spin temperatures [12] by varying the optical pump frequency, which results in inverted, standard, or enhanced Overhauser hyperpolarization buildup and transfer, respectively. Polarization buildup results for these three conditions are seen in the inset to Fig. 2. As described above, a negative spin temperature, resulting from resonant excitation of D^0X transitions 3 and 4, generates enhanced ^{31}P nuclear polarization and the greatest number of nuclear spins able to flip-flop with the ^{29}Si spins.

In contrast, both above-gap and below-gap nonresonant excitation (here 1047 nm $\approx$ 9551 and 9275.08 cm^{-1}, respectively, labeled AG and BG in the inset of Fig. 2) can generate hot conduction band electrons which produce standard Overhauser hyperpolarization by partially saturating the ^{31}P electron spins. Above-gap light generates hot electrons directly from the valence band, while nonresonant, below-gap laser light creates hot electrons indirectly by nonresonantly ionizing donors. This "background" nonresonant ionization process is simultaneously present while optically pumping resonant transitions.

By resonantly pumping D^0X lines 5 and 6, we are able to generate a cold nonequilibrium electron spin temperature, and, as seen in the inset of Fig. 2, these excitation conditions give rise to only a very small amount of ^{29}Si polarization. By pumping electrons from $|\uparrow\rangle$ to $|\downarrow\rangle$, we are removing the ^{31}P nuclear spins from the resonance condition that allows the nuclear spin polarization to diffuse to the ^{29}Si. We are, in principle, generating a ^{31}P nuclear Overhauser polarization that drives the spins into the opposite state when compared to resonantly pumping transitions 3 and 4 or driving any nonresonant process. However, because the thermal electron polarization is so large at 1.4 K, this Overhauser process is extremely weak, and it must compete against the ever present nonresonant below-gap ionization that drives an Overhauser polarization in the standard direction. It should be noted that this nonresonant process is also present when resonantly driving transitions 3 and 4, and has the potential to compromise the maximum achievable ^{29}Si nuclear polarization.

The ^{29}Si polarization buildup is more efficient at the peak matching field condition for each of the three optical frequencies used here: namely resonant, above-gap, and below-gap optical frequencies. This indicates that each of the contributing hyperpolarization processes must first hyperpolarize the ^{31}P nuclear spins. Following this, the hyperpolarization diffuses to the ^{29}Si spins; any direct hyperpolarization of the ^{29}Si spins from the donor electron spins under these conditions occurs much more slowly [24]. Additionally, at the peak matching field condition, nonresonant, below-gap laser light has a similar efficiency as above-gap 1047 nm laser light which will generate significantly more carriers. This indicates that the transfer efficiency does not significantly depend upon the number of conduction band electrons. Together, these observations indicate that the ^{31}P nuclear hyperpolarization, however generated, diffuses efficiently through resonant flop-flops between ^{29}Si and ^{31}P nuclei, and not indirectly through conduction band scattering processes such as the RKKY interaction [25].

We are also able to rule out ^{29}Si hyperpolarization via Overhauser dynamic nuclear polarization (DNP) arising from exchange-coupled donor electrons' hyperfine interaction with ^{29}Si spins, as described by Dementyev *et al.* [6]. Such a process would not give rise to the narrow field-matched response seen in Fig. 2, as the continuum (Hz–GHz) of possible exchange couplings would match the ^{29}Si spins' frequencies across a broad range of magnetic fields. Conversely, the matching field condition described here may have contributed to Dementyev *et al.*'s results taken at 2.35 T, a commonly used field for 100 MHz spectrometers that is coincidentally very near the resonant matching condition we have observed for ^{31}P. This may have contributed to the much stronger DNP signal observed in highly doped (and hence linewidth-broadened) Si:P than that of similarly doped Si:Sb, whose matching field condition lies far away from the magnetic field used in their work.

For a fixed hyperpolarization time of 5 min at the matching field, the polarization of the ^{29}Si spins increases nearly linearly with laser intensity as shown in Fig. 3(a), indicating that higher optical intensity could improve the hyperpolarization rate of the ^{29}Si spins. However, this trend will saturate when the creation rate of hyperpolarized ^{31}P nuclear spins matches the diffusion rate between ^{31}P and ^{29}Si nuclear spins at the matching field.

To accurately determine the overall hyperpolarization of the ^{29}Si spins it is sufficient to compare the hyperpolarized and thermal NMR spin signals in the same physical configuration. However, at 4.2 K we were unable to observe any NMR signal from the ^{29}Si thermal polarization after 60 h of hold time in the dark, or any signal decay from a ^{29}Si polarized state after 24 h in

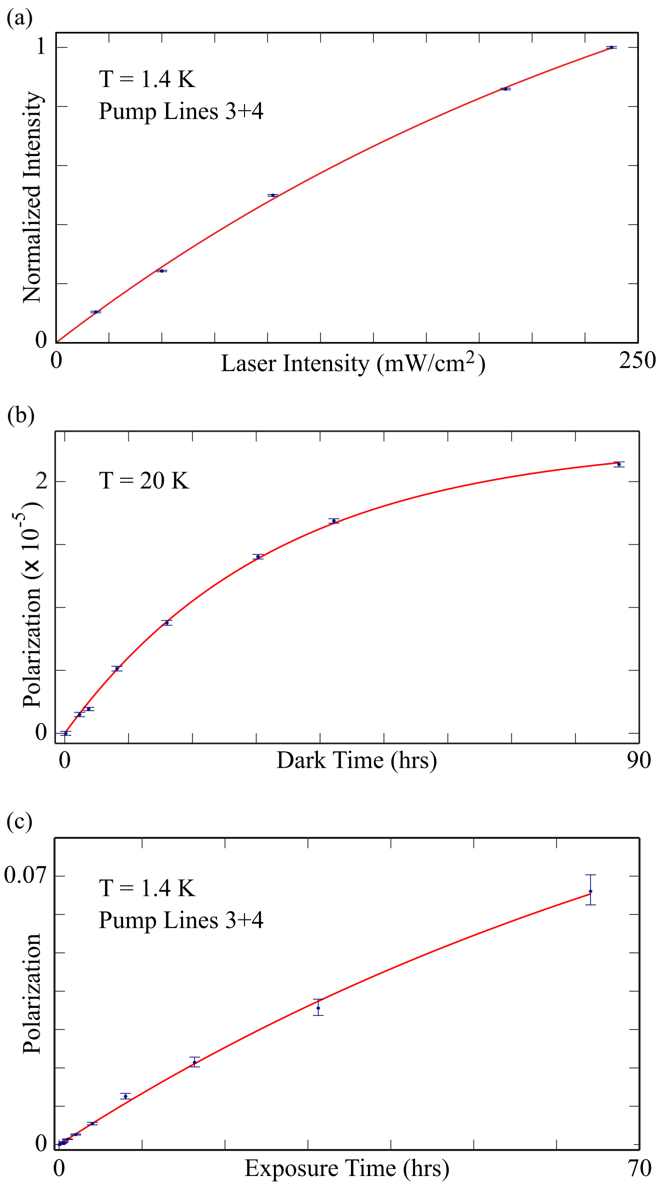

FIG. 3. (Color online) Polarization buildup at $B_0 = 2.2856$ T (a) as a function of laser intensity when exposed for 5 min per point, (b) as a function of hold time in the dark at 20 K, showing the buildup of the equilibrium polarization with a T_1 of ∼33 h, and (c) as a function of exposure time driving optical transitions 3 and 4. We measure a polarization of ∼6.7% for the longest exposure time of 64 h.

the dark, suggesting a very long T_1, making this a challenging prospect to measure directly at the temperatures used in this work. Instead, we recognize that at higher temperatures neutral ^{31}P donors coupled to ^{29}Si centers at the matching field can act as an efficient source of ^{29}Si relaxation as both the donor electron T_1 and the cross-relaxation time are orders of magnitude shorter [26]. At the matching field condition in the dark at 20 K we observe a T_1 polarization buildup time of 33 ± 4 h for the ^{29}Si spins, as seen in Fig. 3(b). We can then use the magnitude of the thermal equilibrium polarization NMR signal at 20 K to infer the total spin polarization of the sample under different conditions.

The polarization buildup as a function of pump time under maximum optical intensity (∼450 mW/cm^2) is shown in Fig. 3(c). We observed a maximum ^{29}Si polarization of $6.7 \pm 0.4\%$ that is still increasing nearly linearly with time even after 64 h. This represents more than a 200 (45 000) fold polarization increase compared to thermal equilibrium at 1.4 K (300 K). A lower-bound estimate of the limiting nuclear hyperpolarization in this all-optical approach, extracted from the exponential fit shown in Fig. 3(c), is $13 \pm 2\%$. However, this value is determined by the Overhauser dynamics of the ^{31}P system and is not an intrinsic limit; with the added complexity of resonant microwave manipulation one could intermix pulsed quantum SWAP operations [16] with the resonant laser excitation used in this experiment to obtain near-unity ^{31}P nuclear polarization iteratively and on demand.

There are a number of possible methods to improve upon the ^{29}Si hyperpolarization rate, which either address the number of resonant hyperpolarized ^{31}P nuclear spins (e.g., by improving the donor electron inversion, increasing the donor concentration, or increasing the rate of ^{31}P hyperpolarization buildup) or consider ways to more efficiently transfer this hyperpolarization from ^{31}P spins to ^{29}Si spins (e.g., using higher donor concentrations [6], dithering the magnetic field over a hyperfine-induced range of matching field conditions, or by resonantly or adiabatically driving a Hartmann-Hahn matching condition [27]). Each combination of these possible future directions still benefits from the core principle of a boosted transfer efficiency from a matching field condition which can later be switched off to regain long T_1 times after hyperpolarization.

These results demonstrate a useful technique for efficiently hyperpolarizing bulk ^{29}Si spins using resonant spin diffusion from the ^{31}P donor nuclei. This technique can be used to efficiently hyperpolarize ^{29}Si spins in micro- and nanoparticle imaging agents, or alternatively "freeze-out" background magnetic field fluctuations from host ^{29}Si nuclear spins for quantum computing applications [28]. Presently, biocompatible silicon MRI agents require a relatively high concentration of surface dangling bonds to efficiently generate Overhauser ^{29}Si nuclear hyperpolarization. Dangling bonds are also the dominant source of ^{29}Si spin relaxation *in vivo*, and can be removed through surface passivation to significantly enhance ^{29}Si T_1 times [10]. It would be advantageous to maximally passivate nanoparticle surfaces to suppress this source of decoherence and instead use the switchable hyperpolarization mechanism identified here to produce long-lived, biocompatible and easily highly hyperpolarized MRI agents.

The work was undertaken at SFU and was supported by the Natural Sciences and Engineering Research Council of Canada (NSERC). For this work S.S. was supported by the Violette and Samuel Glasstone Fellowship and St. John's College, Oxford.

[1] M. C. Cassidy, H. R. Chan, B. D. Ross, P. K. Bhattacharya, and C. M. Marcus, Nat. Nanotech. **8**, 363 (2013).

[2] J. R. Mayo and M. E. Hayden, Radiology **222**, 8 (2002).

[3] J. W. Aptekar, M. C. Cassidy, A. C. Johnson, R. A. Barton, M. Lee, A. C. Ogier, C. Vo, M. N. Anahtar, Y. Ren, S. N. Bhatia, C. Ramanathan, D. G. Cory, A. L. Hill, R. W. Mair, M. S. Rosen, R. L. Walsworth, and C. M. Marcus, ACS Nano **3**, 4003 (2009).
[4] T. D. Ladd, D. Maryenko, Y. Yamamoto, E. Abe, and K. M. Itoh, Phys. Rev. B **71**, 014401 (2005).
[5] H. Hayashi, T. Itahashi, K. M. Itoh, L. S. Vlasenko, and M. P. Vlasenko, Phys. Rev. B **80**, 045201 (2009).
[6] A. E. Dementyev, D. G. Cory, and C. Ramanathan, J. Chem. Phys. **134**, 154511 (2011).
[7] G. Lampel, Phys. Rev. Lett. **20**, 491 (1968).
[8] A. S. Verhulst, I. G. Rau, Y. Yamamoto, and K. M. Itoh, Phys. Rev. B **71**, 235206 (2005).
[9] A. E. Dementyev, D. G. Cory, and C. Ramanathan, Phys. Rev. Lett. **100**, 127601 (2008).
[10] T. M. Atkins, M. C. Cassidy, M. Lee, S. Ganguly, C. M. Marcus, and S. M. Kauzlarich, ACS Nano **7**, 1609 (2013).
[11] A. Abragam, *The Principles of Nuclear Magnetism* (Oxford University Press, Oxford, 1961).
[12] A. Abragam and M. Goldman, Rep. Prog. Phys. **41**, 395 (1978).
[13] E. Hale and R. Mieher, Phys. Rev. **184**, 739 (1969).
[14] A. Yang, M. Steger, T. Sekiguchi, M. L. W. Thewalt, T. D. Ladd, K. M. Itoh, H. Riemann, N. V. Abrosimov, P. Becker, and H. J. Pohl, Phys. Rev. Lett. **102**, 257401 (2009).
[15] D. R. McCamey, J. van Tol, G. W. Morley, and C. Boehme, Phys. Rev. Lett. **102**, 027601 (2009).
[16] S. Simmons, R. M. Brown, H. Riemann, N. V. Abrosimov, P. Becker, H. J. Pohl, M. L. W. Thewalt, K. M. Itoh, and J. J. L. Morton, Nature (London) **470**, 69 (2011).
[17] G. Feher and E. A. Gere, Phys. Rev. **114**, 1245 (1959).
[18] M. Steger, T. Sekiguchi, A. Yang, K. Saeedi, M. E. Hayden, M. L. W. Thewalt, K. M. Itoh, H. Riemann, N. V. Abrosimov, P. Becker, and H. J. Pohl, J. Appl. Phys. **109**, 102411 (2011).
[19] A. Yang, M. Steger, T. Sekiguchi, M. L. W. Thewalt, J. W. Ager, and E. E. Haller, Appl. Phys. Lett. **95**, 122113 (2009).
[20] L. S. Vlasenko, Y. V. Martynov, T. Gregorkiewicz, and C. A. J. Ammerlaan, Phys. Rev. B **52**, 1144 (1995).
[21] K. Saeedi, S. Simmons, J. Z. Salvail, P. Dluhy, H. Riemann, N. V. Abrosimov, P. Becker, H. J. Pohl, J. J. L. Morton, and M. L. W. Thewalt, Science **342**, 830 (2013).
[22] S. Saikin and L. Fedichkin, Phys. Rev. B **67**, 161302 (2003).
[23] G. R. Khutsishvili, Sov. Phys. Usp. **8**, 743 (1966).
[24] G. Feher, Phys. Rev. Lett. **3**, 135 (1959).
[25] K. Yosida, Phys. Rev. **106**, 893 (1957).
[26] T. Castner Jr., Phys. Rev. **130**, 58 (1963).
[27] S. Hartmann and E. Hahn, Phys. Rev. **128**, 2042 (1962).
[28] D. J. Reilly, J. M. Taylor, J. R. Petta, C. M. Marcus, M. P. Hanson, and A. C. Gossard, Science **321**, 817 (2008).